Characteristics of the rotor R4-02 for the O4 NCal system VIR-0661A-22

Eddy Dangelser, Dimitri Estevez, Hubert Kocher, Benoit Mours,
Mehmet Ozturk, Antoine Syx

IPHC-Strasbourg

June 28, 2022

Contents

1   Introduction

This note follows the same discussion made on the rotor R4-01 in VIR-0591A-22. The drawings and figures of the rotor can be found in this technical note.

The rotor has been engraved IPHC-R4-02 on one side and sandblasted on the other side.

2   Measurement method

To determine the geometry of the rotor we will use the same method as for R4-01 (see VIR-0591A-22). The thickness was measured using 24*2 = 48 points (see fig. 1), the outer diameter was measured in 4*2 = 8 points and the inner diameter using 4 points.
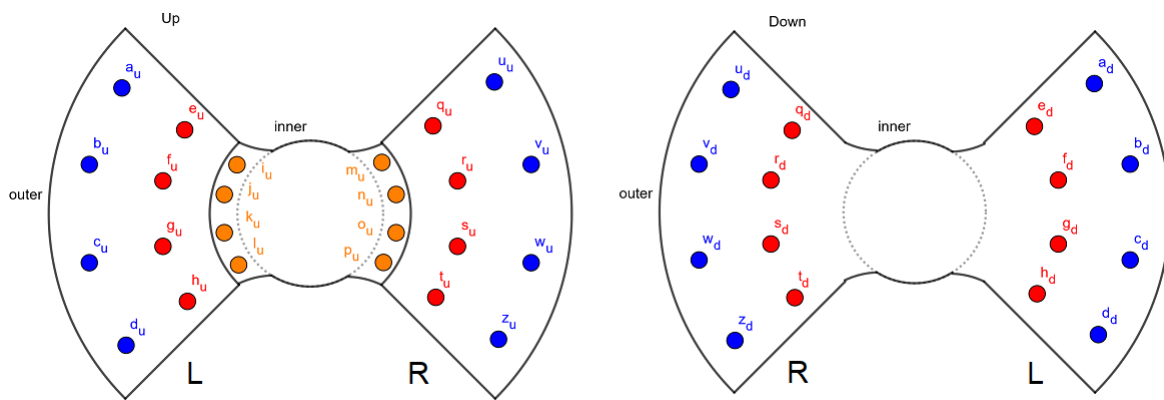

Figure 1: Outline of the faces of the rotor with the measurement points. Left figure is face up, right figure is face down. Sectors have been labelled L for left sector and R for right sector.

The tool used to measure the thickness and the outer diameter is a measuring column "DIGIMAR CX1" (see VIR-0160A-22) with a given precision of $2+L/600$ μm (L the measured length in mm). A vernier caliper "TESA-CAL IP67" with a precision of 20 μm was used to measure the inner diameter.

The measuring column is operated on the same metrology table than the first rotor. The flatness of the surface was estimated to be 2.0 μm (rms of the measurements).

2.1   Thermal effects and density

The rotor R4-02 has been machined from the same aluminum block as R4-01 described in VIR-0160A-22. As for R4-01 the results will be expressed at a reference temperature of 23°C. The density of the rotor R4-02 is then 2808.1 ± 0.2 kg.m^{-3}. This density is measured in air, if the rotor is used under vacuum, the density should be increased by the air density (ρ_{air}=1.3 kg.m^{-3}).

3   Raw measurements of the rotor

This section presents the raw measurements made on the rotor at the ambient temperature of 20.8°C. Table 1 shows the thickness measurements according to the measurement points defined in figure 1. The rotor is laying on the table. The rotor surface as well as the table are not perfectly flat. Some space could be present in between that should be substracted when computing the rotor thickness as discussed later.

Measurement point	L sector		Measurement point	R sector	
	Up	Down		Up	Down
a	104.293	104.256	q	104.292	104.287
b	104.294	104.264	r	104.297	104.291
c	104.301	104.275	s	104.306	104.296
d	104.311	104.289	t	104.314	104.305
e	104.293	104.269	u	104.291	104.287
f	104.293	104.272	v	104.302	104.301
g	104.298	104.279	w	104.315	104.314
h	104.306	104.286	z	104.315	104.326
i	101.586		m	101.577	
j	101.585		n	101.576	
k	101.582		o	101.573	
l	101.582		p	101.575	

Table 1: Raw measurements of the height in mm for each point at 20.8°C on L and R sectors of R4-02.

Table 2 displays the diameter measurements. The measurements were made on 4*2 diameters (two parts of each diameter, the up and down sides of the rotor).

Measurement point	Up	Down
1	207.986	208.016
2	208.025	208.023
3	208.021	208.028
4	208.008	208.016

Table 2: Raw measurements of the diameter in mm for each point at 20.8°C on R4-02.

Measurements were made on the inner radius r_{min} = 28.99 mm and the up face radius for the counterweight $r_{counterweight}$ = 39.99 mm. These values were measured using the vernier caliper and are the same for a temperature of 23°C.

4   Extracting the geometrical parameters

4.1   Thickness

We need to correct the possible gap between the rotor and the measuring table. Assuming that the table is flatter than the rotor surface we can extract the gap from the measurement of the top surface considering the plane tangents to the highest points (asking them to be on both sectors). For this rotor these points are d, w and z from fig. 1. Using the measurements in table 1 we can compute a plane equation for each side of the rotor in cartesian coordinates:

$$\text{Up plane equation} : z = 2.80 \times 10^{-5}x - 1.08 \times 10^{-5}y + 104.31 \tag{1}$$

$$\text{Down plane equation} : z = 2.52 \times 10^{-4}x - 4.82 \times 10^{-4}y + 104.28 \tag{2}$$

Using eqs. (1) and (2) the gap can be determined, see table 3. The maximum rms of the gap for each sector is 11 μm.

Measurement point	L sector		Measurement point	R sector	
	Up	Down		Up	Down
a	17	-14	q	21	-6
b	16	-10	r	17	1
c	9	-5	s	8	7
d	0	0	t	0	6
e	18	-12	u	23	-8
f	18	-7	v	13	-4
g	13	-4	w	0	0
h	5	1	z	0	0

Table 3: Gap computed in μm on up and down sides of both sectors of R4-02.

We can then compute the rotor thickness for each point by removing these gaps. If one of the raw values is lower than the corrected thickness we take this lowest value. The value of each point is shown in table 4 at 23°C.

Measurement point	L sector	Measurement point	R sector
a	104.261	q	104.291
b	104.269	r	104.296
c	104.280	s	104.301
d	104.294	t	104.310
e	104.274	u	104.288
f	104.277	v	104.304
g	104.284	w	104.319
h	104.291	z	104.320
i	101.591	m	101.582
j	101.590	n	101.581
k	101.587	o	101.578
l	101.587	p	101.580

Table 4: Measurements of the thickness in mm for each point at 23°C on L and R sectors of R4-02.

4.2 Radius

Using comparators while the rotor is rotating on its axis we can determine the deformation on both sectors and compute different radii values. Table 5 shows the raw measurements using comparators on L and R sectors. The measurements were made on the up, center and down sides of L and R sectors using three comparators for a total of 5*3*2=30 points (the first and last points are near the edge of the sectors).

Measurement point	L sector			R sector		
	Up	Center	Down	Up	Center	Down
A	0	0	-5	-10	-5	-5
B	20	20	20	15	10	20
C	20	20	20	30	20	20
D	20	20	20	20	15	20
E	0	0	0	0	0	-5

Table 5: Raw measurements in μm of the comparators for the L and R sectors of R4-02.

The zeroing of the comparators was made arbitrarily close to the edge of the sector. The offsets shown in table 5 are measured relative to this reference.

To compute the radius per measurement point we use the following process: First we compute the mean deformation for one comparator. Then we remove this mean deformation to each measurement of this comparator. The corrected shift value is added to the mean radius of 104.013 mm computed using table 2 at 23°C. This process is repeated for each comparator. The final radius for each point are shown in table 6.

Measurement point	L sector			R sector		
	Up	Center	Down	Up	Center	Down
A	103.996	103.998	103.992	103.986	103.993	103.992
B	104.016	104.018	104.017	104.011	104.008	104.017
C	104.016	104.018	104.017	104.026	104.018	104.017
D	104.016	104.018	104.017	104.016	104.013	104.017
E	103.996	103.998	103.997	103.996	103.998	103.992

Table 6: Radius measurements in mm at 20.8°C for the L and R sectors of R4-02.

5 Characterization of the rotor using a simple model

5.1 Theoretical model of the rotor

As explained in VIR-0591A-22 the theoretical strain of the mirror at 2f using FROMAGE v1r2 with the rotor design parameters:

$$\text{strain(2f)} = \frac{2.1198 \times 10^{-18}}{(2f_{rot})^2}$$

This strain value will be compared to models based on the measurements of the rotor.

5.2 Thickness

A simple model can be used to determine a mean value for the thickness and its uncertainty.

As shown on fig. 1, a total of 16 points were used to compute the thickness of each sector. In this case we will not consider the inner points so that we obtain uniform sectors.

For the simple model we take the thickness as the mean value of table 4: 104.292 mm at 23°C. Since we have a limited number of measurement points, to be conservative we take the thickness uncertainty as the rms of table 4 (17.0 μm) to which we add linearly the metrology table uncertainty (2 μm) and the tool uncertainty (2.2 μm). Therefore, for this simple model, the thickness is 104.292 ± 0.021 mm.

5.3 Radius

For the simple model we take the radius as the mean value of table 6: 104.013 mm at 23°C. Using a linear sum of the rms of table 6 (11.5 μm) and the tool uncertainty (2.4 μm) we take an uncertainty of 14 μm on the mean radius.

We have to point out that we do not take into account the fact that the sectors might not be centered on the same axis. Therefore the uncertainty might be underestimated. We will then consider each sector individually later.

5.4 Expected NCal signal and uncertainties

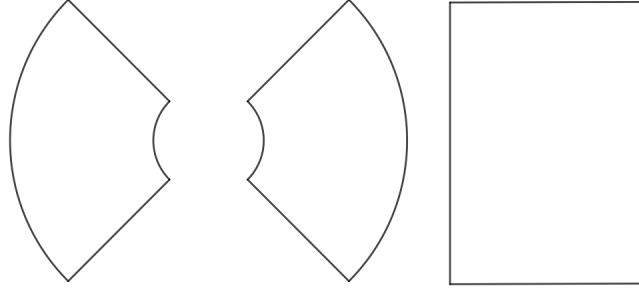The geometry used to describe the rotor as a simple model is represented in figure 2.

Figure 2: Simple model geometry used to describe the rotor. Left is a front view, right is a side view.

Using the analytical equation of the strain at 2f (see eq.8 in Newtonian calibrator tests during the Virgo O3 data taking) we compute with our parameters ($d = 1.7$ m and an angle $\phi = 34.7°$):

$$\text{strain(2f)} = \frac{2.1186 \times 10^{-18}}{(2f_{rot})^2}.$$

Using FROMAGE on this geometry we compute the following 2f strain on the mirror at a distance of 1.7m and an angle of 34.7°:

$$\text{strain(2f)} = \frac{2.1187 \times 10^{-18}}{(2f_{rot})^2}$$

Comparing the theoretical model strain with the simple model at 2f using FROMAGE we obtain a relative deviation of 0.052%.

Comparing the analytical strain at 2f with FROMAGE we obtain a relative deviation of 0.005%.

The uncertainties considered for this model are displayed in table 7.

R4-02 rotor parameter simple model (23°C)			NCal 2f signal uncertainty	
name	value	uncertainty	formula	value (%)
Density ρ (kg.m^{-3})	2808.1	0.2	$\delta\rho/\rho$	0.007
Thickness b (mm)	104.292	2.1×10^{-2}	$\delta b/b$	0.020
r_{max} (mm)	104.013	1.4×10^{-2}	$4\delta r_{max}/r_{max}$	0.053
G (m^3.kg^{-1}.s^{-2})	$6.674\,30 \times 10^{-11}$	1.5×10^{-15}	$\delta G/G$	0.002
Temperature T (°C)	23	3	$\left\|\frac{\partial h}{\partial T}\right\| \frac{\Delta T}{h}$	0.014
Total uncertainty from the rotor (quadratic sum)				0.059

Table 7: Uncertainties on the amplitude of the calibration signal at 2f from the R4-02 rotor simple model geometry. The uncertainties from the opening angles are not included.

6 Characterization of the rotor using an advanced model

6.1 Thickness

A more advanced model can be used considering the deformations on the surfaces of the sectors for better accuracy. Each measurement point of table 4 can be considered as a sub-sector with its own thickness.

The uncertainty on this value is more complex to evaluate. As a conservative approach we use the maximum rms of the deviation to a plane for each sector (11 μm see section 4.1) to which we add linearly the uncertainty on the flatness of the measurement table (2.0 μm) as well as the measurement tool (2.2 μm). The total uncertainty on the thickness is 15 μm.

6.2 Radius

On fig. 1 we divided the external sectors in 4 sub-sectors for each sector (blue points). We convert the point of table 6 to the grid of fig. 1 by averaging the two closest values and converting them to 23°C. The results are shown in table 8. We notice that the L sector is on average 1 μm larger than the R sector.

Radius	L sector			R sector		
	Up	Center	Down	Up	Center	Down
1	104.012	104.013	104.010	104.004	104.006	104.010
2	104.022	104.023	104.023	104.024	104.018	104.023
3	104.022	104.023	104.023	104.027	104.021	104.023
4	104.012	104.013	104.013	104.012	104.011	104.010

Table 8: Radius measurements (in mm at 23°C) for the L and R sectors of R4-02.

The maximum rms of the radii for each sector is 7.7 μm. The tool uncertainty is 2.4 μm. Like for the thickness we use a linear sum and find the uncertainty on both radii to be 10 μm.

6.3 Counterweight

A counterweight has been designed to reduce the unbalance of the rotor. This counterweight is made of aluminum 2017 ($\rho_{Al_{2017}} = 2790$ kg.m^{-3}) and the geometry is shown in fig. 3. The unbalance was nearly a factor 10 smaller than for R4-01, the counterweight was therefore easier to produce.

The dimensions of the counterweight are: an inner radius of 10 mm, an outer radius of 40 mm and a material cut with a chord of 48.65 mm to balance the rotor (see hatched are on fig. 3).
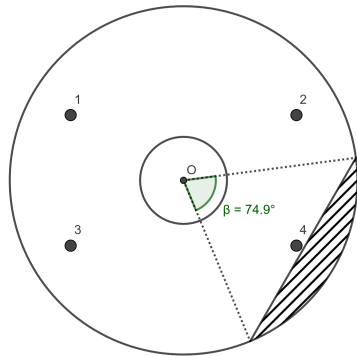

Figure 3: Outline of the counterweight for R4-02. The hatched area represents the material removed.

6.4 Expected NCal signals and uncertainties

6.4.1 Advanced geometry including chamfers and counterweight

The geometry used to describe the rotor as an advanced model is represented in figure 4. The external parts of the sectors are divided in 3 sub-sectors each to correspond to the different radii determined. In addition we include the counterweight, the screws and screw holes.
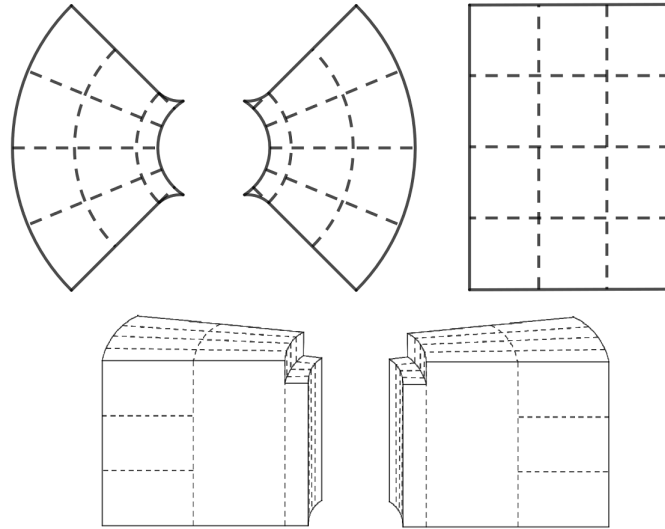
Figure 4: Advanced model geometry used to describe the rotor. Top left is a front view, top right is a side view (external sub-sectors) and bottom is a tilted view of the sectors. Only the 4 external part sectors are divided in 3 sub-sectors each. The chamfers are visible on the inner radius.

Using FROMAGE on this geometry gives the following strains:

- strain(1f) $= \dfrac{3.2167 \times 10^{-21}}{(1 f_{rot})^2}$

- strain(2f) $= \dfrac{2.1180 \times 10^{-18}}{(2 f_{rot})^2}$

- strain(3f) $= \dfrac{1.9337 \times 10^{-23}}{(3 f_{rot})^2}$

The relative deviation to the simple model at 2f is 0.033%.

6.4.2 Opening angles and sectors asymmetry

The counterweight is supposed to compensate the unbalance of the rotor at 1f. As the 1f signal from section 6.4.1 is a bit more than a factor 24 smaller than R4-01 we will consider an error of 0.047%/24=0.002% on the 2f signal for R4-02 due to the opening angle and asymmetry.

6.4.3 Uncertainties

Comparing the advanced model of the rotor + chamfers + screw holes (strain(2f) $= 2.1180 \times 10^{-18}/(2 f_{rot})^2$) to the simple model gives a relative deviation of 0.033%. This deviation will be considered as our modelling uncertainty.

The uncertainties considered for this full model are displayed in table 9.

R4-02 rotor parameter advanced model (23℃)			NCal 2f signal uncertainty	
name	mean value	uncertainty	formula	value (%)
Density ρ (kg.m^{-3})	2808.1	0.2	$\delta\rho/\rho$	0.007
Thickness b left sector (12 sub-sectors) (mm)	104.279	1.5×10^{-2}	$\delta b/b$	0.015
Thickness b right sector (12 sub-sectors) (mm)	104.304			
r_{max} left sector (12 ext sub-sectors) (mm)	104.017	1.0×10^{-2}	$4\delta r_{max}/r_{max}$	0.039
r_{max} right sector (12 ext sub-sectors) (mm)	104.016			
G (m^3.kg^{-1}.s^{-2})	$6.674\,30 \times 10^{-11}$	1.5×10^{-15}	$\delta G/G$	0.002
Temperature T (℃)	23	3	$\left\|\dfrac{\partial h}{\partial T}\right\|\dfrac{\Delta T}{h}$	0.014
Modelling Uncertainty				0.033
Opening angle and asymmetry uncertainty				0.002
Total uncertainty from the rotor (quadratic sum)				0.055

Table 9: Uncertainties on the amplitude of the calibration signal at 2f from the R4-02 rotor advanced model geometry at 23℃.

A   Appendix

```
### This is a cfg file for a more realistic geometry of the mirror and the Virgo NCal for O4 (2022)

### ALL THE OBJECTS ARE DEFINED IN THE MIRROR'S FRAME (O,x,y,z),
### with O the center of the mirror, x axis along the ITF's beam toward the beam-splitter,
### y axis orthogonal to x in the plane of the ITF,
### z axis orthogonal to the plane of the ITF upward


### MIRROR DEFINITION

GRID_SIZE 12 30 8

CYLINDER 2202. 0 0.175 0.2 360 0 0 0

GRID_SIZE 1 1 1

# Defining the flats on the edge of the mirror
CUT_CYL 2202. 0.175 0.2 0.05 0 0
CUT_CYL 2202. 0.175 0.2 0.05 0 180

# Defining the ears and anchors of the mirror
CUBOID 2202. 0.090 0.010 0.015  0      0.1782 -0.0125
CUBOID 2202. 0.090 0.010 0.015  0     -0.1782 -0.0125
CUBOID 2202. 0.039 0.008 0.008 -0.02 -0.1772 -0.024
CUBOID 2202. 0.039 0.008 0.008 -0.02  0.1772 -0.024
CUBOID 2202. 0.039 0.008 0.008  0.02 -0.1772 -0.024
CUBOID 2202. 0.039 0.008 0.008  0.02  0.1772 -0.024

### ROTOR DEFINITION: CYLINDER DENSITY INNER_RADIUS OUTER_RADIUS THICKNESS OPEN_ANGLE r z theta

ROTOR_CYLINDRICAL 1.7 34.7 0 0

### COUNTERWEIGHT 2790.
GRID_SIZE 16 65 40
CYLINDER 2790. 0.010 0.040 0.003 360 0 0.049605 0
GRID_SIZE 1 1 1
CUT_CYL 2790. 0.040 0.002 0.04865 0 330

### SCREW HOLES
GRID_SIZE 4 4 4
CYLINDER -2808.1 0 0.0015 0.012 360 0.03 0.04479563717256 150
CYLINDER -2808.1 0 0.0015 0.012 360 0.03 0.04479363706872 30
CYLINDER -2808.1 0 0.0015 0.012 360 0.03 0.04479113693892 210
CYLINDER -2808.1 0 0.0015 0.012 360 0.03 0.044790136887 330

### SCREWS COUNTERWEIGHT
CYLINDER 4810. 0 0.0015 0.003 360 0.03 0.0496049974818 150
CYLINDER 7600. 0 0.0015 0.00665 360 0.03 0.04747063717256 150

CYLINDER 4810. 0 0.0015 0.003 360 0.03 0.0496049974818 30
CYLINDER 7600. 0 0.0015 0.00665 360 0.03 0.04747063717256 30

CYLINDER 4810. 0 0.0015 0.003 360 0.03 0.0496049974818 210
CYLINDER 7600. 0 0.0015 0.00665 360 0.03 0.04747063717256 210
```

```
CYLINDER 4810. 0 0.0015 0.003 360 0.03 0.0496049974818 330
CYLINDER 7600. 0 0.0015 0.00665 360 0.03 0.04747063717256 330


# TRES RAPIDE
#GRID_SIZE 4 4 4
# RAPIDE
#GRID_SIZE 8 17 14
# LENT
GRID_SIZE 8 65 40


### L sector

## Inner part
OUTER_FILLET 2808.1 0.02899 0.101591 -0.002691 0.01 -11.25 146.25
CYLINDER 2808.1 0.02899 0.03999 0.101591 22.5 0 -0.002691 146.25
CYLINDER 2808.1 0.02899 0.03999 0.101590 22.5 0 -0.002692 168.75
CYLINDER 2808.1 0.02899 0.03999 0.101587 22.5 0 -0.002691 191.25
CYLINDER 2808.1 0.02899 0.03999 0.101587 22.5 0 -0.002691 213.75
OUTER_FILLET 2808.1 0.02899 0.101587 -0.002691 0.01 11.25 213.75


## Middle part
CYLINDER 2808.1 0.03999 0.071991 0.104274 22.5 0 0 146.25
CYLINDER 2808.1 0.03999 0.071991 0.104277 22.5 0 0 168.75
CYLINDER 2808.1 0.03999 0.071991 0.104284 22.5 0 0 191.25
CYLINDER 2808.1 0.03999 0.071991 0.104291 22.5 0 0 213.75


## Outer part
CYLINDER 2808.1 0.071991 0.104012 0.03475380432384 22.5 0 0.03475380432384 146.25
CYLINDER 2808.1 0.071991 0.104013 0.03475380432384 22.5 0 0 146.25
CYLINDER 2808.1 0.071991 0.104010 0.03475380432384 22.5 0 -0.03475380432384 146.25

CYLINDER 2808.1 0.071991 0.104022 0.03475647112896 22.5 0 0.03475647112896 168.75
CYLINDER 2808.1 0.071991 0.104023 0.03475647112896 22.5 0 0 168.75
CYLINDER 2808.1 0.071991 0.104023 0.03475647112896 22.5 0 -0.03475647112896 168.75

CYLINDER 2808.1 0.071991 0.104022 0.034760137986 22.5 0 0.034760137986 191.25
CYLINDER 2808.1 0.071991 0.104023 0.034760137986 22.5 0 0 191.25
CYLINDER 2808.1 0.071991 0.104023 0.034760137986 22.5 0 -0.034760137986 191.25

CYLINDER 2808.1 0.071991 0.104012 0.0347647733847103 22.5 0 0.0347647733847103 213.75
CYLINDER 2808.1 0.071991 0.104013 0.0347647733847103 22.5 0 0 213.75
CYLINDER 2808.1 0.071991 0.104013 0.0347647733847103 22.5 0 -0.0347647733847103 213.75


### R sector

## Inner part
OUTER_FILLET 2808.1 0.02899 0.101582 -0.002718 0.01 11.25 33.75
CYLINDER 2808.1 0.02899 0.03999 0.101582 22.5 0 -0.002718 33.75
CYLINDER 2808.1 0.02899 0.03999 0.101581 22.5 0 -0.002719 11.25
CYLINDER 2808.1 0.02899 0.03999 0.101578 22.5 0 -0.002722 348.75
CYLINDER 2808.1 0.02899 0.03999 0.101580 22.5 0 -0.002720 326.25
OUTER_FILLET 2808.1 0.02899 0.101580 -0.002720 0.01 -11.25 326.25


## Middle part
CYLINDER 2808.1 0.03999 0.071991 0.104291 22.5 0 0 33.75
CYLINDER 2808.1 0.03999 0.071991 0.104296 22.5 0 0 11.25
```

```
CYLINDER 2808.1 0.03999 0.071991 0.104301 22.5 0 0 348.75
CYLINDER 2808.1 0.03999 0.071991 0.104310 22.5 0 0 326.25


## Outer part
CYLINDER 2808.1 0.071991 0.104004 0.0347627113273708 22.5 0 0.0347627113273708 33.75
CYLINDER 2808.1 0.071991 0.104006 0.0347627113273708 22.5 0 0 33.75
CYLINDER 2808.1 0.071991 0.104010 0.0347627113273708 22.5 0 -0.0347627113273708 33.75

CYLINDER 2808.1 0.071991 0.104024 0.0347679170081797 22.5 0 0.0347679170081797 11.25
CYLINDER 2808.1 0.071991 0.104018 0.0347679170081797 22.5 0 0 11.25
CYLINDER 2808.1 0.071991 0.104023 0.0347679170081797 22.5 0 -0.0347679170081797 11.25

CYLINDER 2808.1 0.071991 0.104027 0.03477313866096 22.5 0 0.03477313866096 348.75
CYLINDER 2808.1 0.071991 0.104021 0.03477313866096 22.5 0 0 348.75
CYLINDER 2808.1 0.071991 0.104023 0.03477313866096 22.5 0 -0.03477313866096 348.75

CYLINDER 2808.1 0.071991 0.104012 0.0347734379882276 22.5 0 0.0347734379882276 326.25
CYLINDER 2808.1 0.071991 0.104011 0.0347734379882276 22.5 0 0 326.25
CYLINDER 2808.1 0.071991 0.104010 0.0347734379882276 22.5 0 -0.0347734379882276 326.25

### GENERAL PARAMETERS

STEP 22.5 16

ARM_LENGTH 3000

SIGNAL 3
```